

## Review article

# Current status and future potential of computer-aided diagnosis in medical imaging

K DOI, PhD

*Kurt Rossmann Laboratories for Radiologic Image Research, Department of Radiology, The University of Chicago, 5841 South Maryland, MC 2026, Chicago, IL 60637, USA*

**Abstract.** Computer-aided diagnosis (CAD) has become one of the major research subjects in medical imaging and diagnostic radiology. The basic concept of CAD is to provide a computer output as a second opinion to assist radiologists' image interpretation by improving the accuracy and consistency of radiological diagnosis and also by reducing the image reading time. In this article, a number of CAD schemes are presented, with emphasis on potential clinical applications. These schemes include: (1) detection and classification of lung nodules on digital chest radiographs; (2) detection of nodules in low dose CT; (3) distinction between benign and malignant nodules on high resolution CT; (4) usefulness of similar images for distinction between benign and malignant lesions; (5) quantitative analysis of diffuse lung diseases on high resolution CT; and (6) detection of intracranial aneurysms in magnetic resonance angiography. Because CAD can be applied to all imaging modalities, all body parts and all kinds of examinations, it is likely that CAD will have a major impact on medical imaging and diagnostic radiology in the 21st century.

Recently, computer-aided diagnosis (CAD) has become one of the major research subjects in medical imaging and diagnostic radiology [1–13]. Over the last 3 years, at the Annual Meetings of the Radiological Society of North America (RSNA) in Chicago, which is one of the major meetings in the field of diagnostic radiology, the number of papers presented on subjects related to CAD has increased by approximately 50% per year, from 55 in 2000, to 86 in 2001, to 134 in 2002, and 191 in 2003. Many different types of CAD schemes are being developed for detection and/or characterisation of various lesions in medical imaging, including conventional projection radiography, computed tomography (CT), magnetic resonance imaging (MRI) and ultrasound. Organs currently being subjected to research for CAD includes the breast, chest, colon, brain, liver, kidney, and the vascular and skeletal systems.

The basic concept of CAD is to provide a computer output as a "second opinion" to assist radiologists' image readings [1–7]. Therefore, for development of a successful CAD scheme it is necessary not only to develop computer algorithms, but also to investigate how useful the computer output would be for radiologists in their diagnoses, how to quantify the benefits of the computer output for radiologists, and how to maximize the effect of the computer output on their diagnoses. Thus, large-scale observer performance studies on radiologists using a reliable methodology such as receiver operating characteristic (ROC) analysis are equally as important as the development of computer algorithms in the field of CAD. Therefore, the research and development of CAD has involved a team effort by investigators with different backgrounds such as physicists, radiologists, computer scientists, engineers, psychologists and statisticians.

CAD has generally been defined by diagnosis made by a physician who takes into account the computer output

based on quantitative analysis of radiological images. This definition is clearly distinct from automated computerised diagnosis [14–20], which was attempted in the 1960s and 1970s, replacing radiologists by computers. However, our serious investigation of CAD at the University of Chicago began in the 1980s with a clear goal in mind of assisting radiologists by use of a computer. The goal of CAD is to improve the quality and productivity of radiologists' tasks by improving the accuracy and consistency of radiological diagnoses and also by reducing the image reading time. The general approach for CAD is to find the location of a lesion and also to determine an estimate of the probability of a disease; these correspond to CAD for detection of a lesion and CAD for differential diagnosis. The basic technologies involved in CAD schemes are: (1) image processing for detection and extraction of abnormalities; (2) quantitation of image features for candidates of abnormalities; (3) data processing for classification of image features between normals and abnormal (or benign and malignant); (4) quantitative evaluation and retrieval of images similar to those of unknown lesions; and (5) observer performance studies using ROC analysis.

Because the concept of CAD is broad, CAD can be applied to all imaging modalities, including projection radiography, CT, MRI, ultrasound and nuclear medicine imaging, used for all body parts such as the skull, thorax, heart, abdomen and extremities, and all kinds of examinations including skeletal imaging, soft tissue imaging, functional imaging and angiography. However, the majority of CAD schemes developed in the past include the detection of breast lesions on mammograms [7, 21–30], the detection of lung nodules in chest radiographs [31–49] and thoracic CT [50–71], and the detection of polyps in CT colonography [72–82]. Therefore, the current results obtained from basic research and clinical applications of CAD may be considered the tip of an

iceberg, and thus a major impact of CAD on medical imaging and diagnostic radiology may be expected in the future.

One of the important events in the history of CAD is that R2 Technology has succeeded in commercialisation of the first CAD system for detection of breast lesions in mammography based on licensing of CAD technologies from The University of Chicago, and that it obtained US Food and Drug Administration (FDA) approval for the clinical use of their system in 1998. Subsequently, clinical uses of the mammographic CAD system have begun at many screening sites for breast cancer in the United States, and more than 1500 CAD systems are in current use in assisting radiologists in the early detection of breast cancer at many hospitals, clinics and screening centres around the world. It has also been reported that CAD has provided a gain of approximately 20% in the early detection of breast cancers on mammograms [29]. In 2001, Deus Technologies developed another CAD system for detection of lung nodules on chest radiographs, and then received FDA approval for its clinical use. In Japan, Mitsubishi Space Software has developed a CAD system with temporal subtraction of sequential chest radiographs and also for detection of lung nodules on chest images. A number of prototype systems for detection of pulmonary nodules in thoracic CT have been developed by manufacturers and are being evaluated at medical centres around the world. Recently, R2 Technology received FDA approval for their CAD system for detection of pulmonary nodules in CT.

Because a number of commercial CAD systems for detection of breast cancer on mammograms are currently available for clinical use, some recent research on mammographic CAD has been focused on clinical studies evaluating the effect of CAD on radiologists' performance and on clinical outcomes [83–88]; these include prospective studies on the detection rates of breast cancer without and with the use of CAD [29, 89] and comparison of double readings of mammograms with single reading by CAD [90]. At present, the results of these studies are mixed and controversial, thus requiring further investigations on the effect of the computer output on clinical outcome based on prospective studies and/or randomised clinical trials.

The development of multidetector CT (MDCT) has produced a large number of CT images that may require additional time and effort in image interpretation by radiologists. It has been expected, therefore, that CAD would assist radiologists in reducing the reading time as well as in improving the diagnostic accuracy. Many investigators have attempted to develop CAD schemes for detection of pulmonary nodules by MDCT. Because the quality of MDCT images has been improved considerably in terms of three-dimensional (3D) image information over that of conventional CT images with relatively thick slices, the performance of CAD schemes in the detection of nodules on MDCT images has generally been improved.

In this review article, a number of CAD schemes developed at The University of Chicago are presented, with emphasis on potential clinical applications in the future. Subjects for these CAD schemes included in the following sections are: (1) detection and classification of lung nodules on digital chest radiographs; (2) detection

of nodules in low dose CT; (3) distinction between benign and malignant nodules on high resolution CT; (4) usefulness of similar images for distinction between benign and malignant lesions; (5) quantitative analysis of diffuse lung diseases on high resolution CT; and (6) detection of intracranial aneurysms in magnetic resonance angiography.

### Detection and classification of lung nodules on digital chest radiographs

It has been well documented that radiologists may miss approximately 30% of lung nodules on chest radiographs, some of which are clearly visible in retrospect. Therefore, the purpose of CAD for detection of nodules on chest radiographs is to indicate the potential locations of nodules as a prompt to radiologists. The computerised scheme for automated detection of nodules was based on a difference-image technique [31, 32] with which nodules were enhanced and the majority of background normal structures were suppressed. The candidates for nodules were then identified by thresholding of pixel values in the difference image derived from a chest radiograph. A number of image features on nodule candidates were quantified, and some false positives caused by normal anatomical structures were removed by a rule-based method together with the use of an artificial neural network (ANN). Finally, the locations of potential sites for nodules were indicated by markers such as arrows on chest images displayed on a monitor, as illustrated in Figure 1. It is apparent in Figure 1 that a subtle nodule overlapped with a rib in the left lung was correctly detected by the computer, but that one false positive in the computer output which is pointing to a normal anatomical structure in the mediastinum was included. It is important to reduce the number of such false positives as much as possible in all CAD schemes, including that for detection

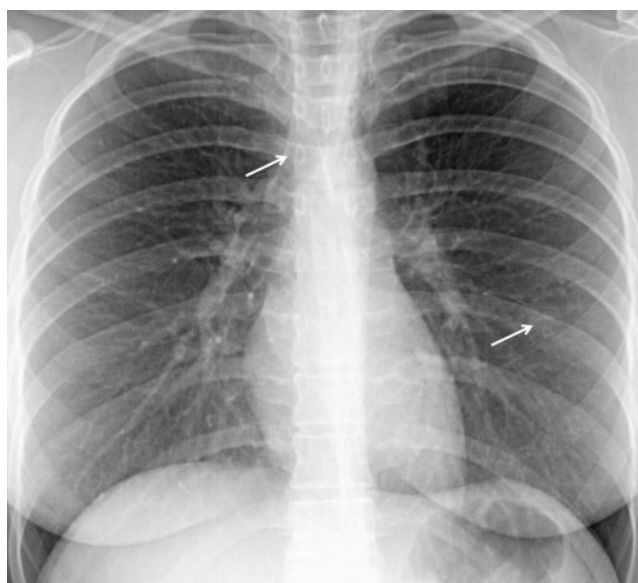


**Figure 1.** Illustration of the computer output marked by two arrows; one indicates the correct detection of a subtle nodule in the left lung, and the other corresponds to a false positive, which is a normal structure in the mediastinum.

of lung nodules. The usefulness of a computer output such as that shown in Figure 1 has been investigated in observer performance studies by use of ROC analysis [33]. Two sets of digital chest radiographs, *i.e.* one without and another with computer output, were presented to radiologists for detection of nodules. Radiologists' performance in detecting nodules on chest radiographs was evaluated in terms of the  $A_z$  value, which is the area under the ROC curve. Results indicated that the  $A_z$  value was improved from 0.894 to 0.940 when the computer output was available. The performance level of the computer output used in this study was a sensitivity of 80% with one false positive per chest image. The difference in  $A_z$  values obtained from the two ROC curves has been confirmed to be statistically significant ( $p=0.001$ ) [33].

Figure 2 shows  $A_z$  values for 16 radiologists, obtained without and with computer output. It is apparent that all of the radiologists were able to improve their detection performance by using of the computer output. Without CAD, the average  $A_z$  value for eight residents was lower than that for attendings. However, the average gain in  $A_z$  value due to CAD was greater for the resident group than for the attending group. Therefore, with CAD the average  $A_z$  value for the eight residents became comparable with that for the eight attendings. These results indicate that CAD can assist many radiologists in improving their accuracy in detecting lung nodules, and also in reducing the variation in detection accuracy due to the variation in radiologists' experience (*i.e.* residents *vs* attendings). Therefore, these results appear to indicate the potential that the purpose of CAD as described above can be realised in improving the accuracy and consistency of radiological diagnoses.

Once a lung nodule is found on a chest radiograph, the subsequent task for a radiologist is to assess the nature of the lesion, *i.e.* whether the nodule is malignant or benign. This task of classification of lung nodules is considered difficult for radiologists. The purpose of CAD for classification of nodules on chest radiographs is to provide the likelihood of malignancy as a second opinion in

assisting radiologists' decisions [47, 48]. The computerised scheme for determination of the likelihood of malignancy is based on the analysis of many image features obtained from a nodule on a chest radiograph and also from the corresponding difference image. The image features include features obtained from the outline of the nodule such as the shape and size, the distribution of pixel values inside and outside the nodule, and the distribution of edge components.

The likelihood measure of malignancy was determined by use of linear discriminant analysis (LDA) or an ANN on a multidimensional distribution of image features. Figure 3 shows the likelihood measure of malignancy for three malignant and three benign nodules. Shiraishi et al [49] have investigated the usefulness of these results for classification of nodules in observer performance studies by use of ROC analysis. Figure 4 shows ROC curves obtained without and with the computer output in distinguishing between benign and malignant nodules on chest radiographs. It is apparent that radiologists' performance in the distinction between benign and malignant nodules was improved significantly by use of the computer output. However, it is important to note that the ROC curve for radiologists with CAD was still lower than that obtained with the computer alone. This result seems to indicate that, although radiologists were able to utilise "some of the computer output" in improving their performance, they could not effectively take full advantage of the computer output. The reasons for this may be related to the present lack of experience with such computer output. Therefore, when radiologists become familiar with CAD for classification of nodules, the benefits obtained with CAD might be increased further.

In addition to the two CAD schemes for detection and classification of lung nodules on chest images as illustrated above, a number of different CAD schemes have been developed for detection of other abnormalities such as interstitial opacities [34–36], cardiomegaly [45], pneumothorax [46] and interval changes [39–44] on chest radiographs as well as for differential diagnosis of

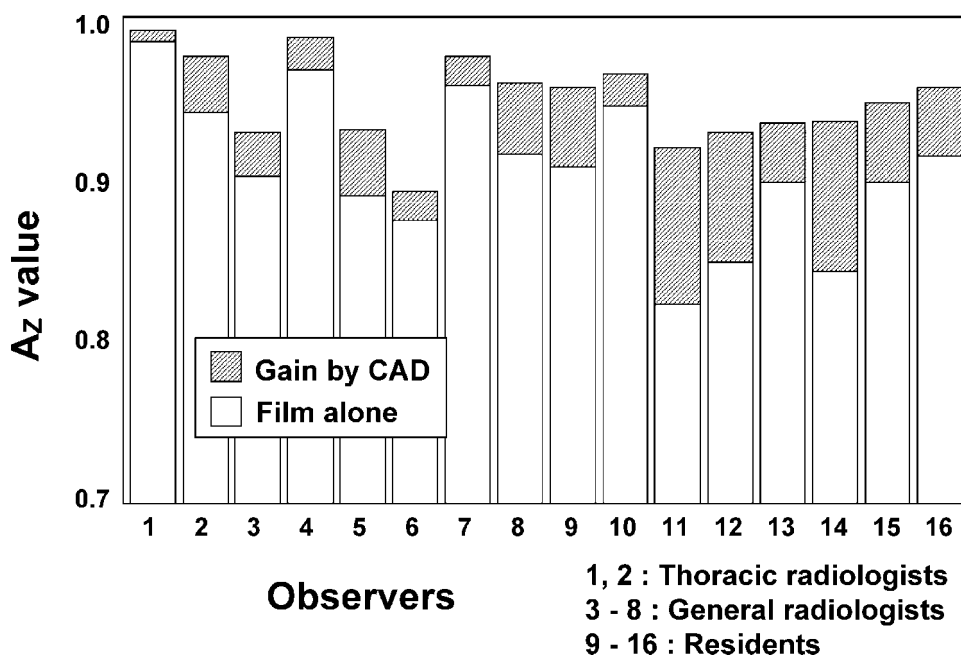


**Figure 2.**  $A_z$  values without and with computer-aided diagnosis (CAD) for 16 radiologists in the detection of lung nodules on chest radiographs. 60 normals and 60 abnormal with lung nodules of varying subtlety were used.

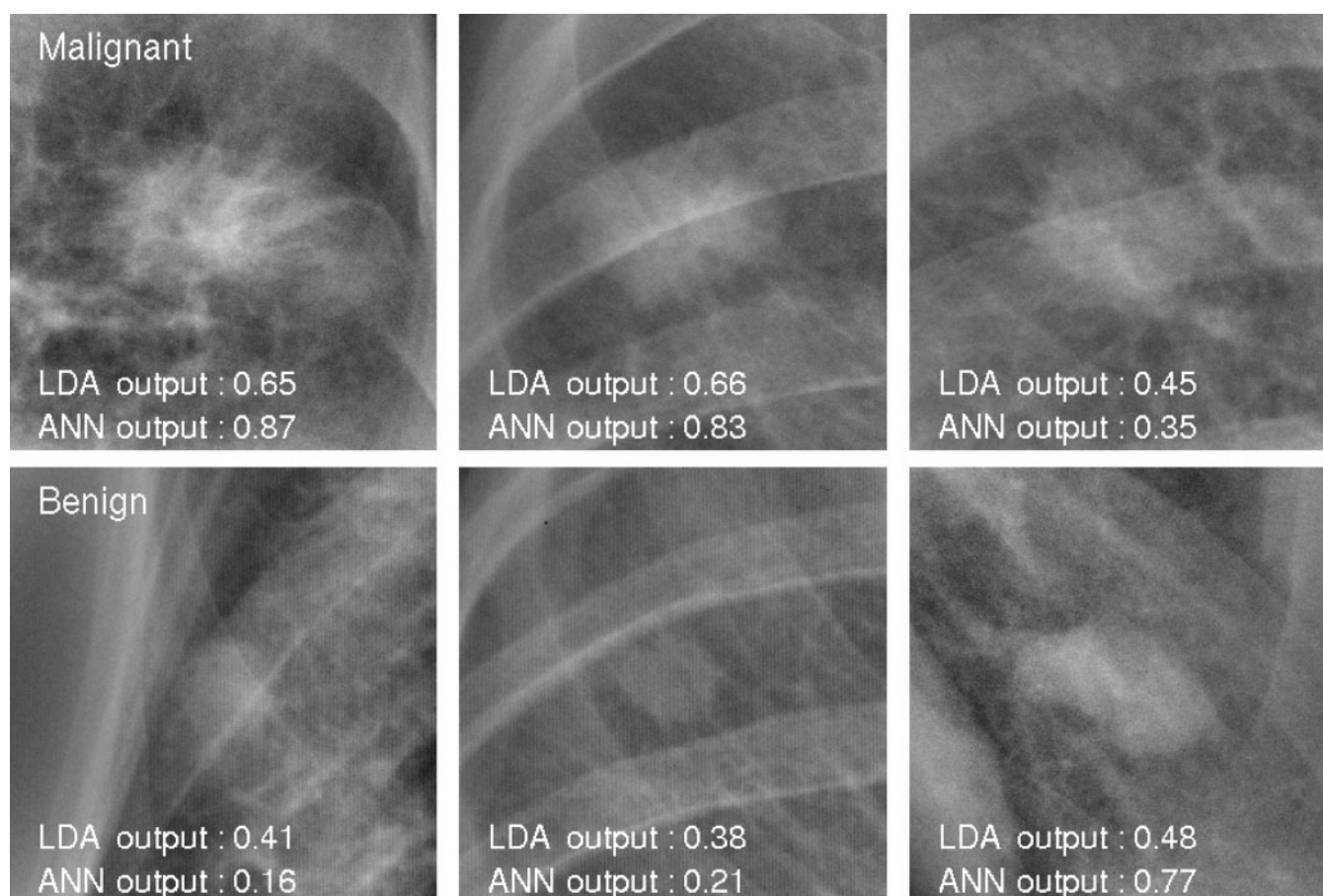


**Figure 3.** Illustration of malignant and benign nodules on chest radiographs together with the likelihood measure of malignancy obtained with a computer-aided diagnosis (CAD) scheme by use of linear discriminant analysis (LDA) and on artificial neural network (ANN). A computer output above or below 0.50 indicates the likelihood of malignancy or benignancy, respectively.

interstitial lung disease [37, 38]. The potential usefulness of these CAD schemes has been demonstrated in a number of observer performance studies using ROC analysis [36, 38, 42–44, 91]. Therefore, when newer digital chest systems such as flat-panel detectors and computed radiography systems are installed in a hospital in the future, it is very likely that a package of software providing various prompts for potential abnormalities will be installed in a computer associated with the image acquisition system and/or picture archiving and communication system (PACS).

### Detection of pulmonary nodules on low dose CT

Low dose helical computed tomography (LDCT) screening is regarded as one of the most promising techniques for early detection of lung cancer [92–101]. It has been reported that CT images are superior to chest radiographs for detecting peripheral lung cancers [92]. However, it is a difficult and time consuming task for radiologists to detect subtle lung nodules in a large number of CT slices for lung cancer screening. Thus, a CAD scheme would be useful for assisting radiologists in cancer screening using LDCT. A number of investigators [50–71] have attempted to develop CAD schemes for computerised detection of lung nodules using various methods and techniques.

Arimura et al [102] have developed a CAD scheme based on a difference-image technique for enhancing lung nodules and suppressing the majority of background normal structures. The difference image for each CT image was obtained by subtraction of the nodule-suppressed image processed with a ring average filter from the nodule-enhanced image with a matched filter. The initial nodule candidates were identified by application of a multiple grey level thresholding technique to the difference image, where most nodules were enhanced well. A number of false positives were removed first from the entire lung, and then from the selected lung regions by use of two rule-based schemes on the localised image features related to morphology and grey levels. Some of the remaining false positives were eliminated by use of a multiple massive training artificial neural network (MTANN), which was trained for reduction of various types of false positives.

Suzuki et al [60, 103] have developed the MTANN consisting of a modified multilayer ANN, which is capable of operating on the original image directly, as illustrated in Figure 5. The MTANN was trained by use of a large number of subregions extracted from input images together with teacher images containing the distribution for the “likelihood of being a nodule”. The output image was obtained by scanning an input image with the MTANN. The distinction between a nodule and a non-nodule was made by use of a score that was defined from

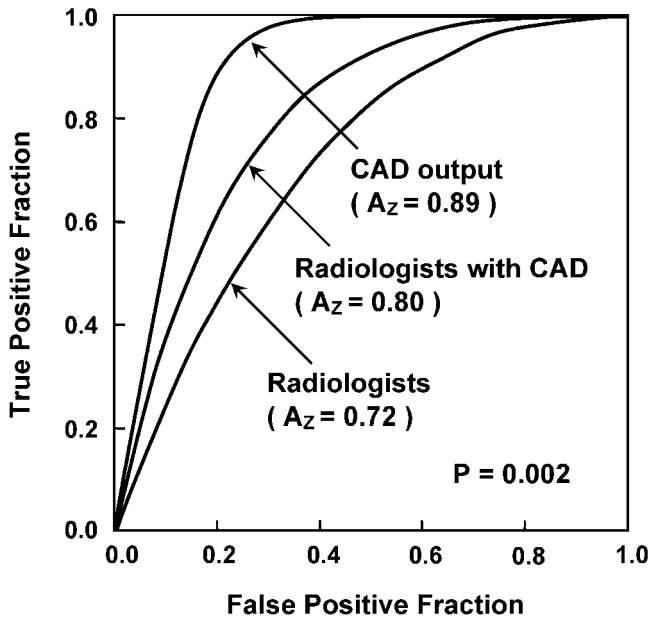


**Figure 4.** Receiver operating characteristic (ROC) curves for distinction between malignant and benign nodules, on chest radiographs without and with the computer-aided diagnosis (CAD) outputs such as those shown in Figure 3. 16 radiologists participated in an observer study in the interpretation of 53 chest radiographs, including 31 primary lung cancers and 22 benign nodules.

the output image of the trained MTANN. The multi-MTANN for eliminating various types of non-nodules consisted of a number of MTANNs arranged in parallel. Each MTANN was trained by use of the same nodules but with a different type of false positive, such as various-sized

vessels, and acted as an expert to distinguish nodules from a specific type of false positive. The outputs of the MTANNs were combined by use of the logical AND operation, so that each of the trained MTANNs did not eliminate any nodules but removed some of the various types of false positives. Our computerised scheme was applied to a confirmed cancer database of 106 LDCT scans with 109 cancer lesions in 73 patients obtained from a lung cancer screening program [93] in Nagano, Japan. Our CAD scheme provided a sensitivity of 83% (91/109) for all cancers with 5.8 false positives per scan, which included 84% (32/38) for missed cancers with 5.9 false positives per scan.

The usefulness of the MTANN in removing a large number of false positives in a CAD scheme is illustrated in Figure 6. The number of false positives per scan was reduced from 27.9 to 12.5 by use of a single MTANN, and further reduced to 3.8 by use of multiple MTANNs, thus substantially improving the performance of the CAD scheme. Another unique advantage of the MTANN is related to a relatively small number of training cases required for the MTANN compared with that for a conventional ANN. A single MTANN can be trained by use of only 10 nodules and 10 false positives. However, because each of the training cases is scanned 500 000 times, the total number of iterations for training becomes several billions, which is the reason for referring to this ANN as a “massive training” ANN. Therefore, the CPU (central processing unit) time for training the MTANN can be quite long, for example 30 h [60, 103], whereas the trained MTANN can provide the output almost instantly.

Figure 7 shows the computer output that correctly detected “missed” cancers [52, 101] in the Nagano

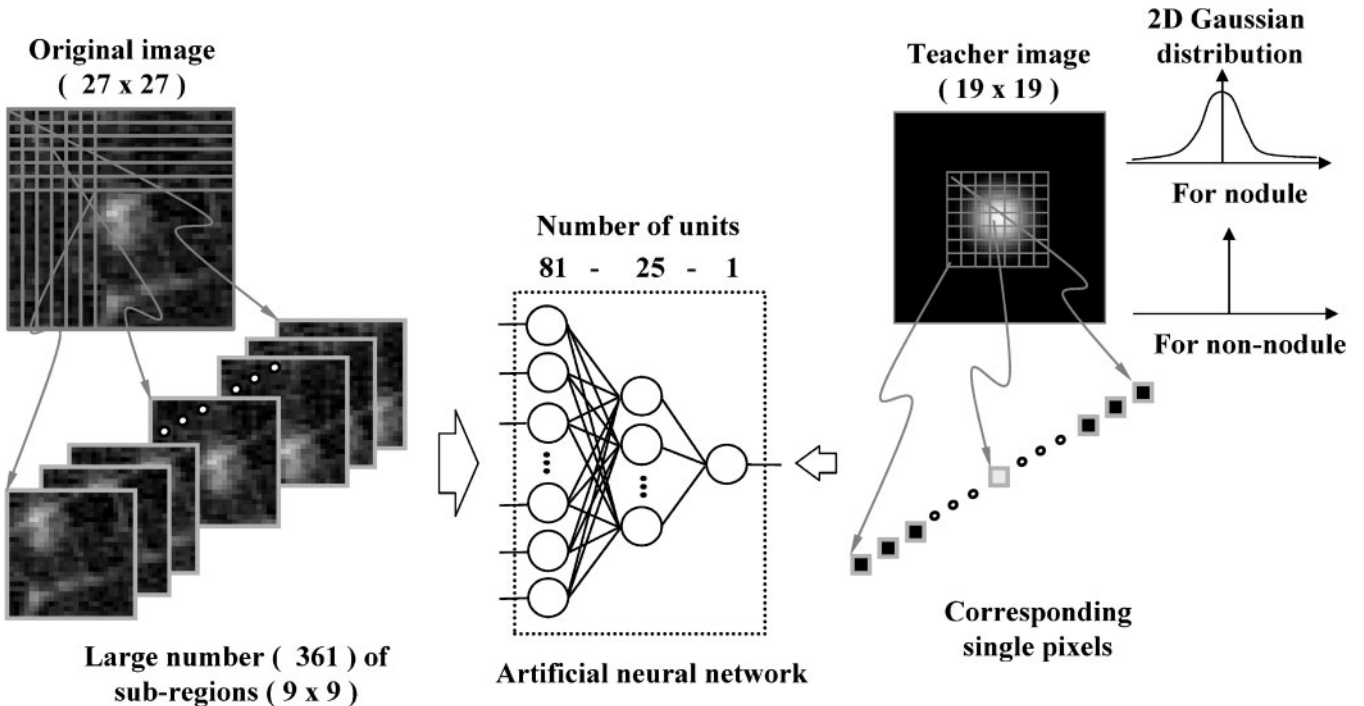


**Figure 5.** Illustration of the basic structure of a massive training artificial neural network (MTANN) together with image data as input and teacher image data as output, used for training the MTANN. Typically, 10 nodules and 10 false positives are used for training a single MTANN.

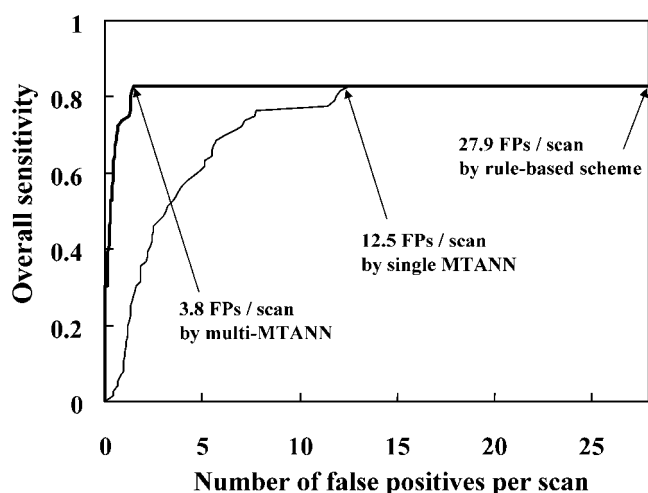


**Figure 6.** Illustration of the usefulness of the massive training artificial neural network (MTANN) in reducing the number of false positives (FPs) in computerised detection of nodules in low dose CT (LDCT) images. Single MTANN or multi-MTANN was applied to a rule-based computer-aided diagnosis (CAD) scheme for 63 LDCT scans with 71 nodules including 66 primary cancers and 5 benign nodules.

database, which had been identified retrospectively as “actionable” lesions 1 or 2 years prior to the diagnosis of cancer in the screening programme. These missed cancers were generally considered very subtle and appeared as small, faint nodules, overlapping normal structures or opacities in a complex background caused by other disease [101]. Li et al [104] have used these “missed” cancer cases for observer performance study by selection of normal cases by matching age, gender and smoking status to the cancers from the same screening programme. Observer studies were carried out with CT images displayed on an LCD (liquid-crystal display) monitor using the cine mode, where the sensitivity of the CAD scheme for detection of these cancer cases was 80% and the average number of false positives was 2.7 per case. Figure 8 shows ROC curves for radiologists without and with the computer output in detecting these missed cancers [104], where the  $A_z$  value was improved from 0.755 to 0.845 ( $p=0.03$ ) by use of the computer output. It is important to note that lung cancers missed at CT screening were very difficult to detect even in an observer study. However, our CAD scheme improved radiologists’ performance in detecting these subtle cancers, despite the fact that the performance level of the computer was much lower than that of radiologists alone. This improvement in radiologists’ performance was possible because radiologists were able to disregard the majority of false positives and were reminded of some of their oversight by the correct computer output.

### Likelihood of malignancy for pulmonary nodules on high resolution CT

CT screening has led to early detection of peripheral lung cancer and also to detection of a large number of false positives (*i.e.* non-calcified benign nodules) [92–94, 98, 99]. The false positive rate at screening has been reported as 87–93% with low dose, single detector CT

at 10 mm slice thickness [92–94], and 98–99% with single detector or multidetector CT at 5 mm slice thickness [98, 99]. Also, simultaneous or additional diagnostic high resolution CT (HRCT) is needed for distinction between lung cancers and benign nodules detected as suspicious or indeterminate lesions by screening CT [92–94, 98, 99]. This high false positive rate due to benign nodules is likely to reduce the benefit of CT screening for early detection of lung cancer [100]. It is therefore important to differentiate benign from malignant nodules to reduce the false positives for screening CT, and also to reduce follow-up examinations for diagnostic HRCT.

Aoyama et al [105] have developed an automated computerised scheme for determination of the likelihood measure of malignancy by using various objective features of the nodules in our database of thick section, low dose screening CT, where one or two slices were employed for image analysis on each nodule. Recently, we further developed another computerised scheme for distinction between malignant and benign lesions by using more than 50 objective features derived from multiple slices of diagnostic HRCT obtained from low dose CT screening. Li et al [106] have carried out observer performance studies using ROC analysis for evaluation of the effectiveness of our CAD scheme to assist radiologists in distinguishing benign from malignant small nodules in various patterns at HRCT. The lung cancers included nodules with pure ground-glass opacity (GGO), mixed GGO and solid opacity, as illustrated in Figure 9, whereas benign nodules were selected by matching their size and pattern to the cancers on HRCT in this observer study.

Consecutive region-of-interest (ROI) images for each nodule on HRCT were displayed for interpretation in cine mode on a CRT (cathode ray tube) monitor. The images were presented to 16 radiologists, first without and then with the computer output, to indicate their confidence level regarding the malignancy of a nodule. The resulting ROC curves are shown in Figure 10, where the  $A_z$  value of the CAD scheme alone was 0.831 for distinguishing benign from malignant nodules. The average  $A_z$  value for radiologists was improved from 0.785 to 0.853 by a statistically significant amount ( $p=0.016$ ) with the aid of the CAD scheme [106]. In addition, it is important to note that the radiologists’ performance with the CAD scheme was better than that of the CAD scheme alone ( $p<0.05$ ), and also better than that of the radiologists alone. One may ask why this is possible. From a detailed analysis of radiologists’ responses and computer outputs, we found that radiologists were correct and the computer output was incorrect in some cases, whereas the computer was correct and the radiologists were incorrect in other cases. Therefore, the radiologists’ overall performance was improved by maintaining their “firm” correct decisions on some cases and by correcting their initial mistakes by looking at the computer output on other cases. This is a synergistic effect of the computer and radiologists: all of CAD is intended eventually to produce multiplicative benefits by humans and computer. Thus, CAD has the potential to improve diagnostic accuracy in distinguishing small benign nodules from malignant ones on HRCT.

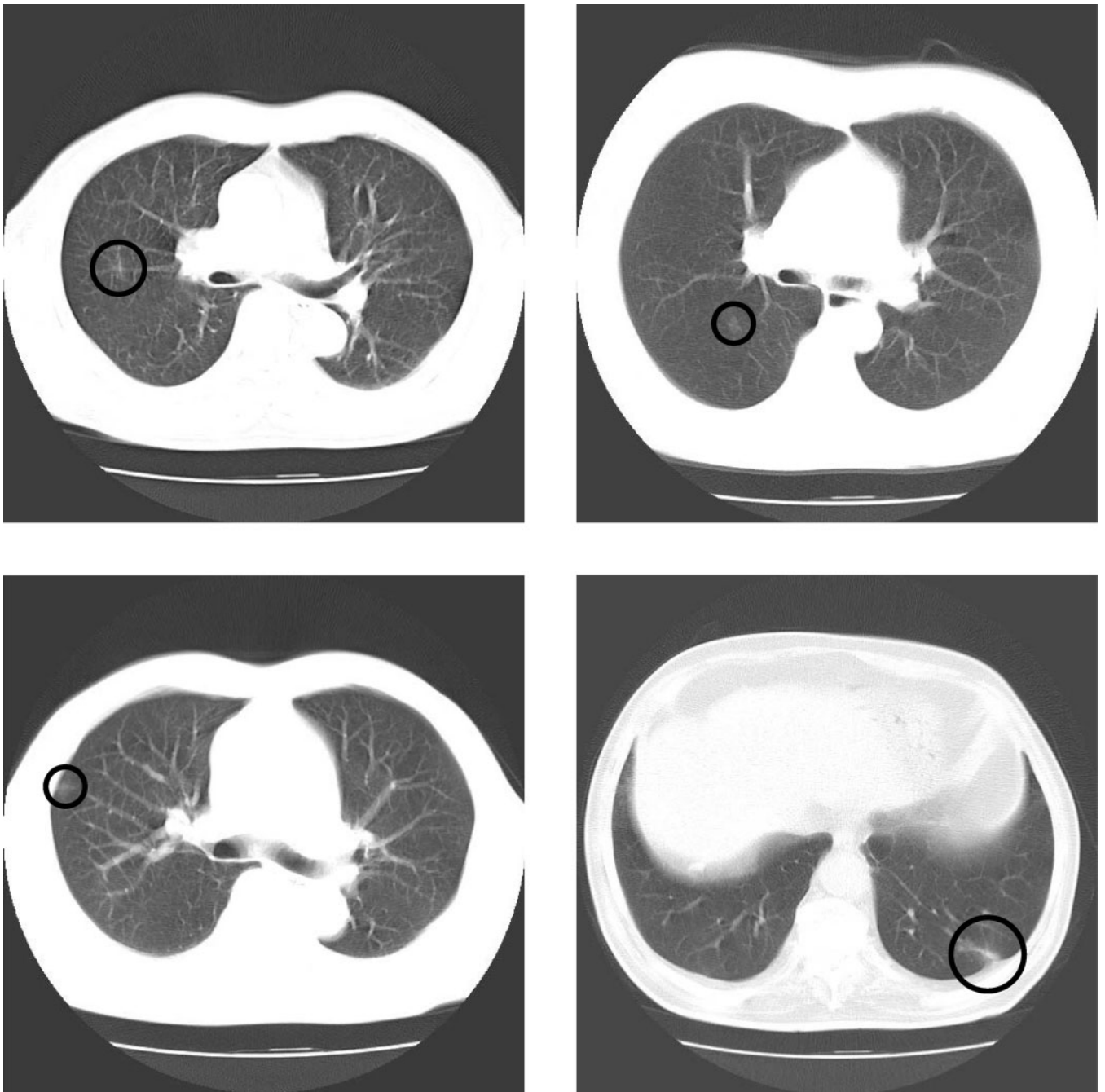


**Figure 7.** Illustration of subtle missed cancers, which were detected correctly by our computer-aided diagnosis (CAD) scheme, on low dose CT images obtained from a lung cancer screening.

### **Usefulness of similar images for distinction between benign and malignant nodules on low dose CT**

To assist radiologists in differential diagnosis, it may be useful to provide a set of benign and malignant images that are similar to an unknown new case in question. If the new case were considered by a radiologist to be very similar to one or more benign (or malignant) images, then s/he would be more confident in deciding that the new case is benign (or malignant). Therefore, similar images may be employed to supplement the computed likelihood of malignancy for implementing CAD for differential diagnosis. The usefulness of similar images has been

demonstrated in an observer performance study [107], in which the  $A_z$  value in the distinction between benign and malignant modules in thoracic CT was improved. Figure 11 illustrates the comparison of an unknown case of a pulmonary nodule in the centre with three benign cases on the left and three cases with malignant nodules on the right, which were obtained from LDCT used in a lung cancer screening programme [93, 108, 109] in Nagano, Japan. It has been confirmed that most radiologists were able to identify the unknown case correctly as being more similar to malignant nodules than to benign ones.

The reason for presenting similar images is based on the fact that radiologists learn diagnostic skills by observing many clinical cases during their training and clinical

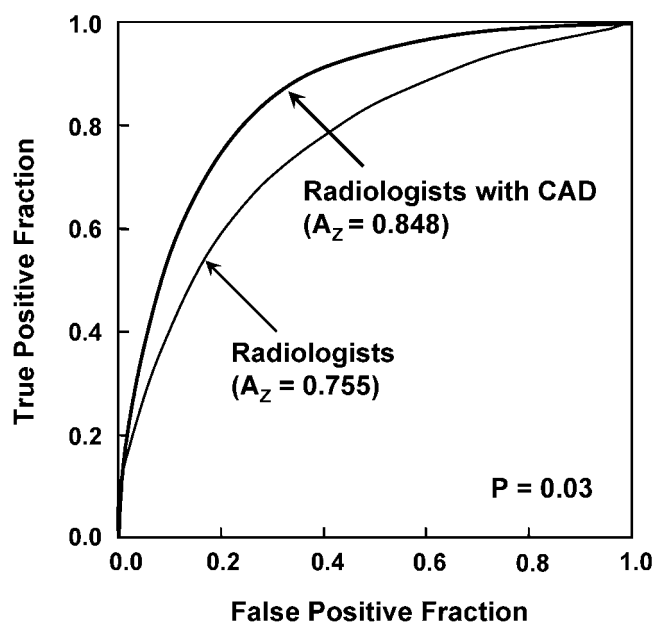


**Figure 8.** Receiver operating characteristic (ROC) curves without and with computer-aided diagnosis (CAD) output for detection of lung cancers in low dose CT images. Six radiologists participated in an observer study, detecting missed peripheral lung cancers in 27 cases including 17 CT scans with cancer and 10 CT scans without cancer.

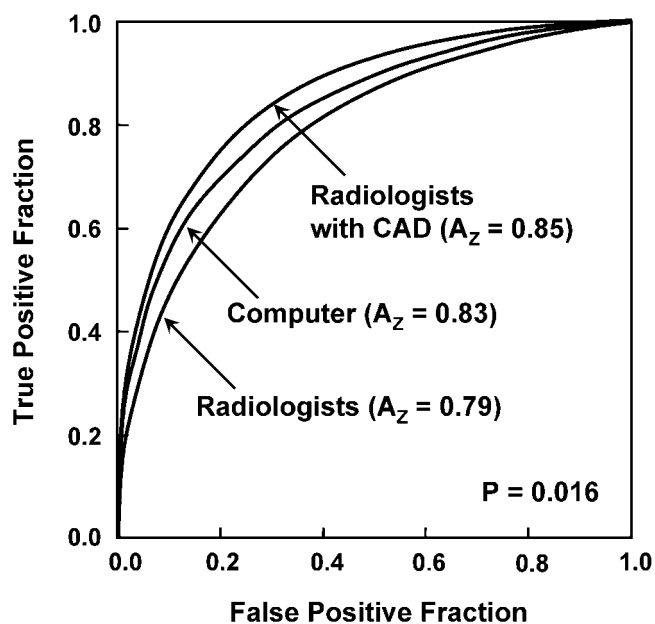


**Figure 10.** Receiver operating characteristic (ROC) curves without and with computer-aided diagnosis (CAD) output for distinction between malignant and benign nodules on high resolution CT. The images used in this study included 28 primary lung cancers (6–20 mm) and 28 benign nodules that were selected by matching their size and pattern to the cancers. A ROC curve for the computer results is also shown.

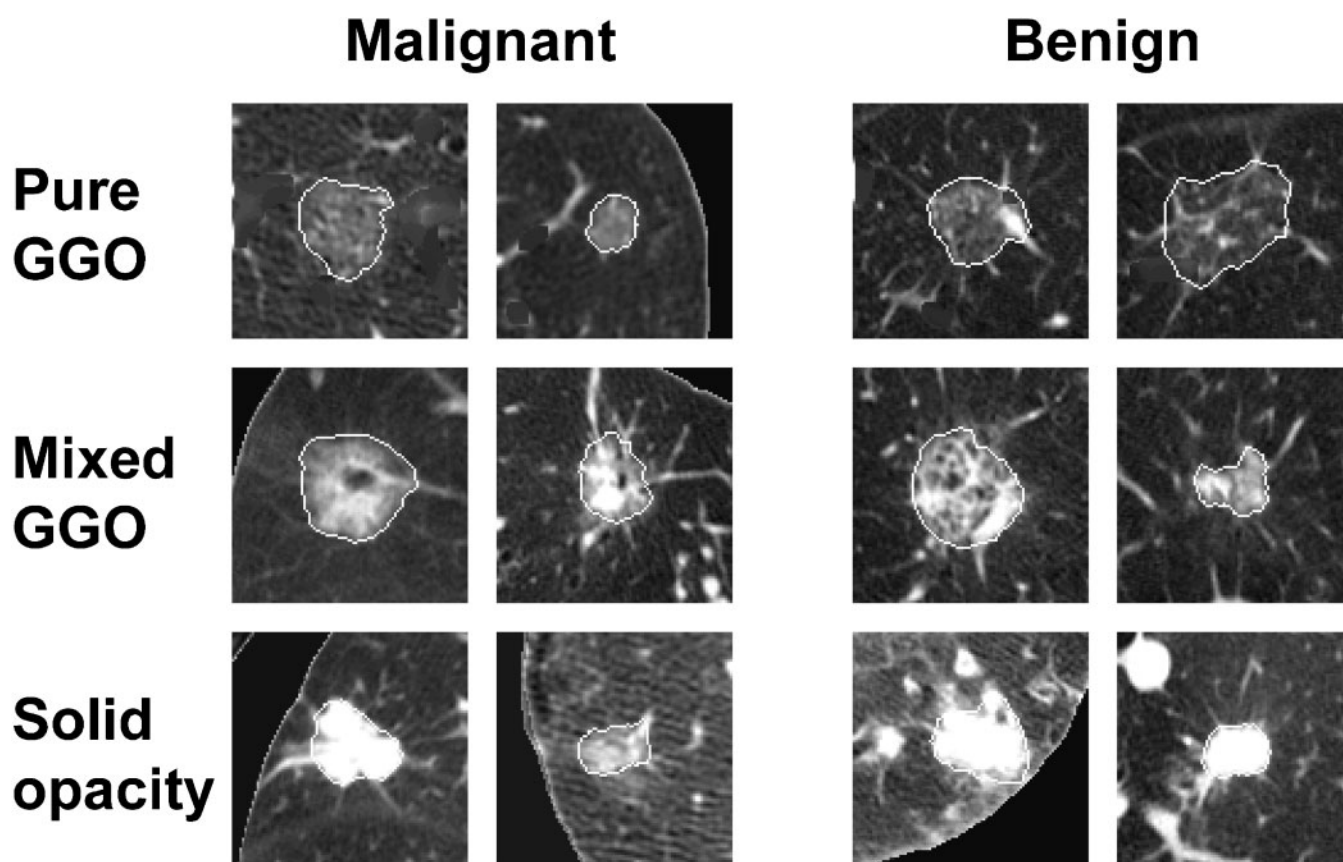


**Figure 9.** Illustration of malignant and benign nodules with pure ground-glass opacity (GGO), mixed GGO and solid opacity. These nodules were segmented for subsequent analysis for determination of the likelihood measure of malignancy.

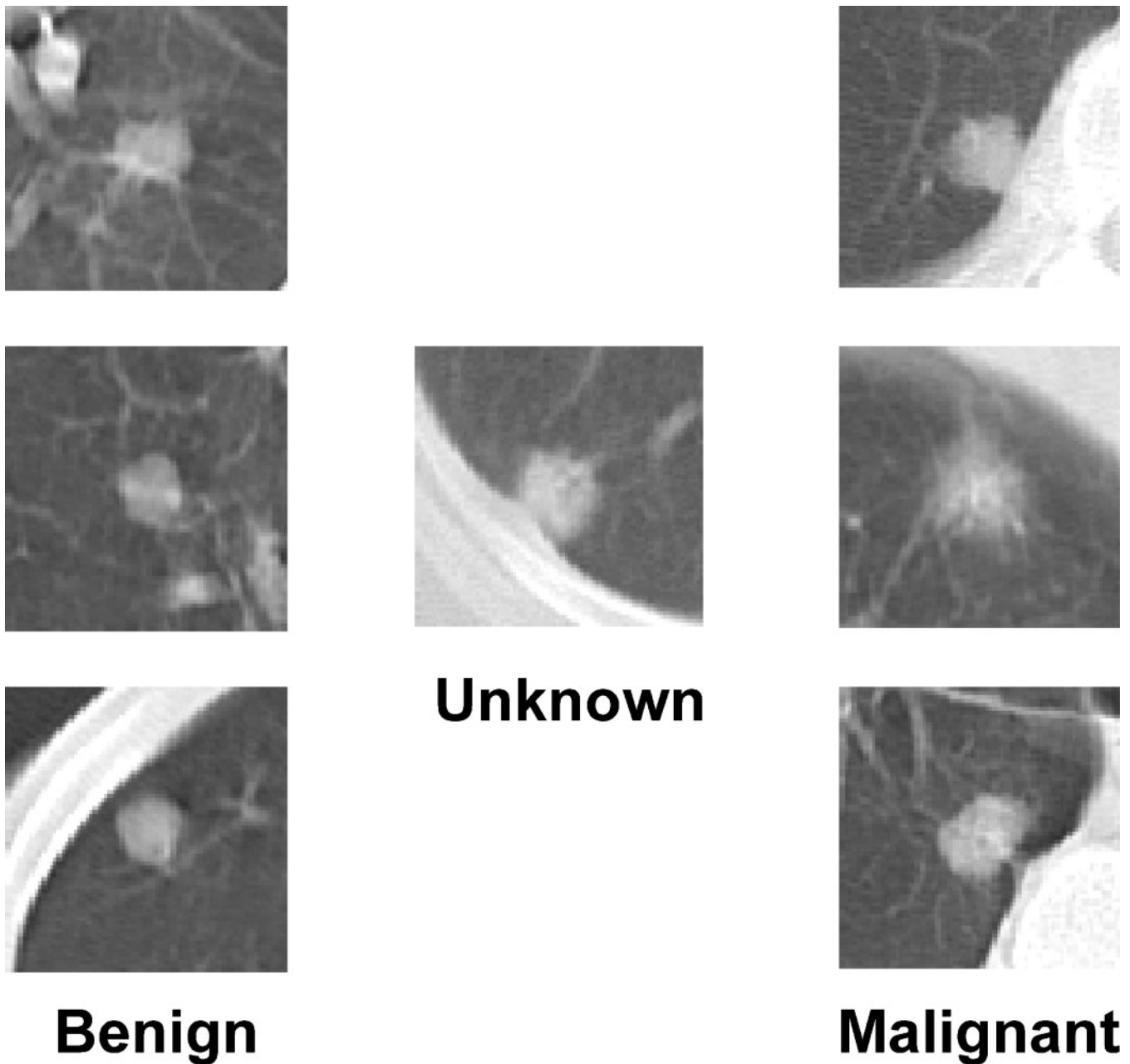


**Figure 11.** Illustration of the potential usefulness of similar images for distinction between malignant and benign lesions. The image in the centre is an unknown case on low dose CT, and two sets of benign and malignant nodules that would be similar to the unknown case are shown on the left and right, respectively.

practice, and their knowledge obtained from visual impression of images with various diseases constitutes the foundation for their diagnosis. Two fundamental issues related to the concept of similar images are: (1) how radiologists perceive the similarity between two nodules subjectively; and (2) how one can determine a reliable similarity measure that would agree well with the subjective similarity according to radiologists' judgement. If "similar" nodules determined by a computerised scheme are not really similar to the unknown nodule in terms of radiologists' visual perception, these nodules would not be useful in assisting radiologists in the diagnosis of an unknown nodule.

However, it would be very difficult to develop a reliable and useful method for quantifying the similarity of a pair

of images (or lesions) for visual comparison by radiologists. For example, for a given pair of lesions when most of the measurable objective features such as size, shape and contrast of the two lesions are almost identical, two lesions may appear to a radiologist to be similar visually based on the diagnosis of benign lesions; however, two lesions may look very different to the radiologist if one of the lesions contains a very subtle spiculation indicating malignancy. It is also possible that, even when most of the objective features are quite different, two lesions will look very similar to radiologists if the two lesions contain only one common feature such as subtle localised spiculations, localised sharp edges or non-uniform densities. Therefore, it would be very difficult to define a reliable measure for the similarity of lesions based on objective image features

alone. It would be necessary to take into account both objective features and subjective judgement on the similarities for many pairs of lesions in formulating a useful measure for selection of similar lesions in a database.

Recently, Li et al [107] conducted an observer study to obtain subjective rating data by radiologists on the similarity of a large number of pairs of pulmonary nodules in LDCT images. They employed an ANN to learn the relationship between objective features and subjective ratings on pairs of nodules. The ANN was trained by use of objective features for pairs of nodules as the input data, and the corresponding subjective similarity rating as the teacher data. The trained ANN was used as a tool to provide a new psychophysical similarity measure for objective features of a given pair of nodules, which were entered as input data. Li et al [107] demonstrated a high correlation value of 0.72 for the relationship between psychophysical measures and radiologists' subjective ratings; this appears to be a promising development.

There is another important issue related to the use of similar images in practical clinical situations, that is the need for a unique database that includes a large number of images which can be used as being similar to those in many unknown new cases. Although it may take

considerable time, a database for this purpose can be developed in the future.

### Quantitative analysis of diffuse lung diseases on HRCT

The differential diagnosis of diffuse lung disease is a major subject in HRCT. However, it is considered a difficult task for radiologists, partly because of the complexity and variation in diffuse disease patterns on HRCT images, and also because of the subjective terms used for describing diffuse lung diseases. Therefore, our goal was to develop a CAD scheme [110] for diffuse lung diseases on HRCT to assist radiologists' image interpretation as a "second opinion".

In an initial study [110], we attempted to determine physical measures on HRCT images in order to detect and characterise diffuse lung diseases, which will be the basis for application to the differential diagnosis of diffuse lung disease in the future. We compared the physical measures of normal slices with those of abnormal slices, which included six typical patterns of diffuse lung diseases. In addition, we investigated the classification performance for distinction between normal and abnormal slices. Our database consisted of 315 HRCT images selected from 105

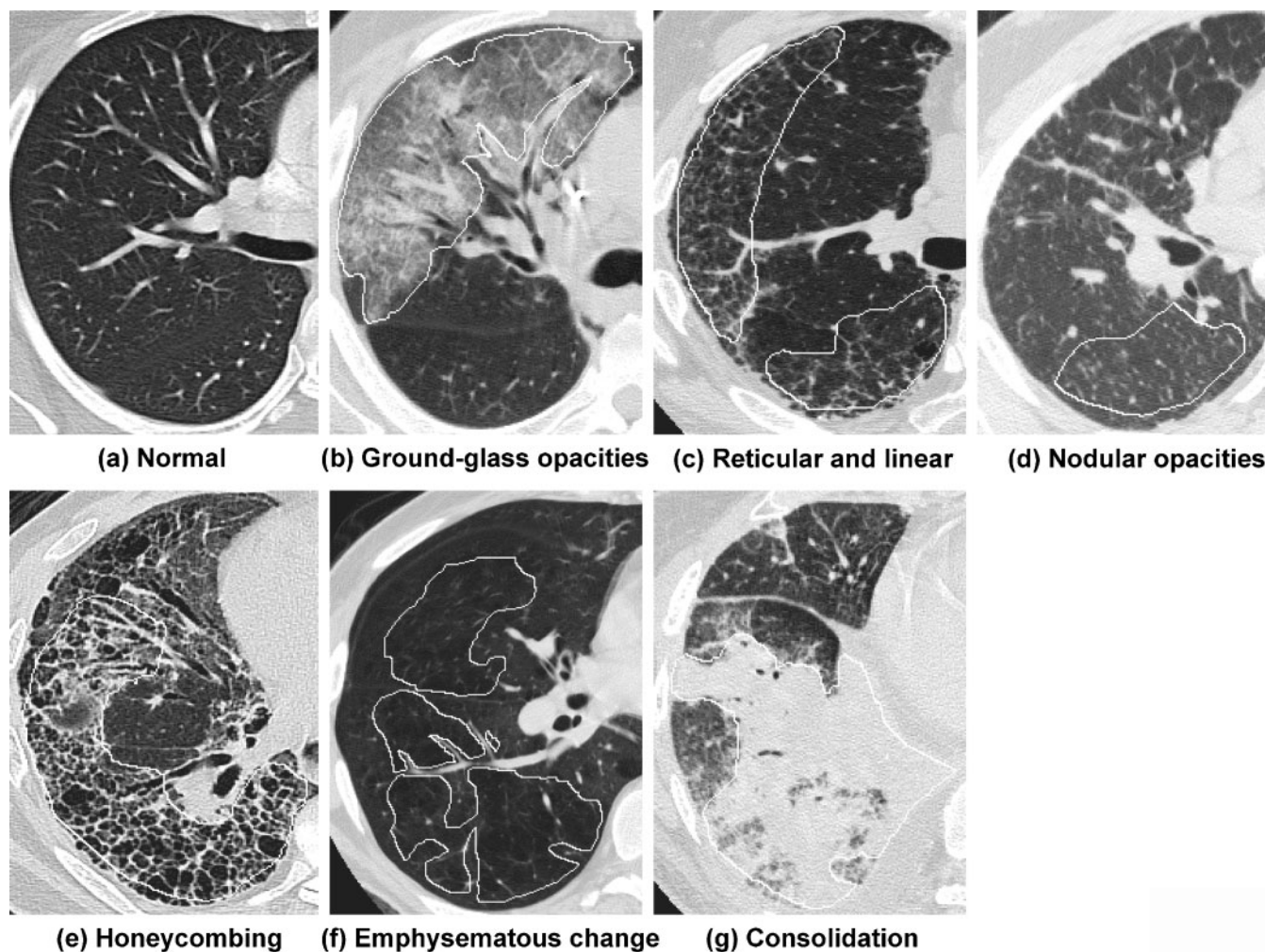


**Figure 12.** Illustration of "gold standard" for one normal and six abnormal patterns of diffuse lung diseases on high resolution CT images that were determined by the areas marked independently by three radiologists.

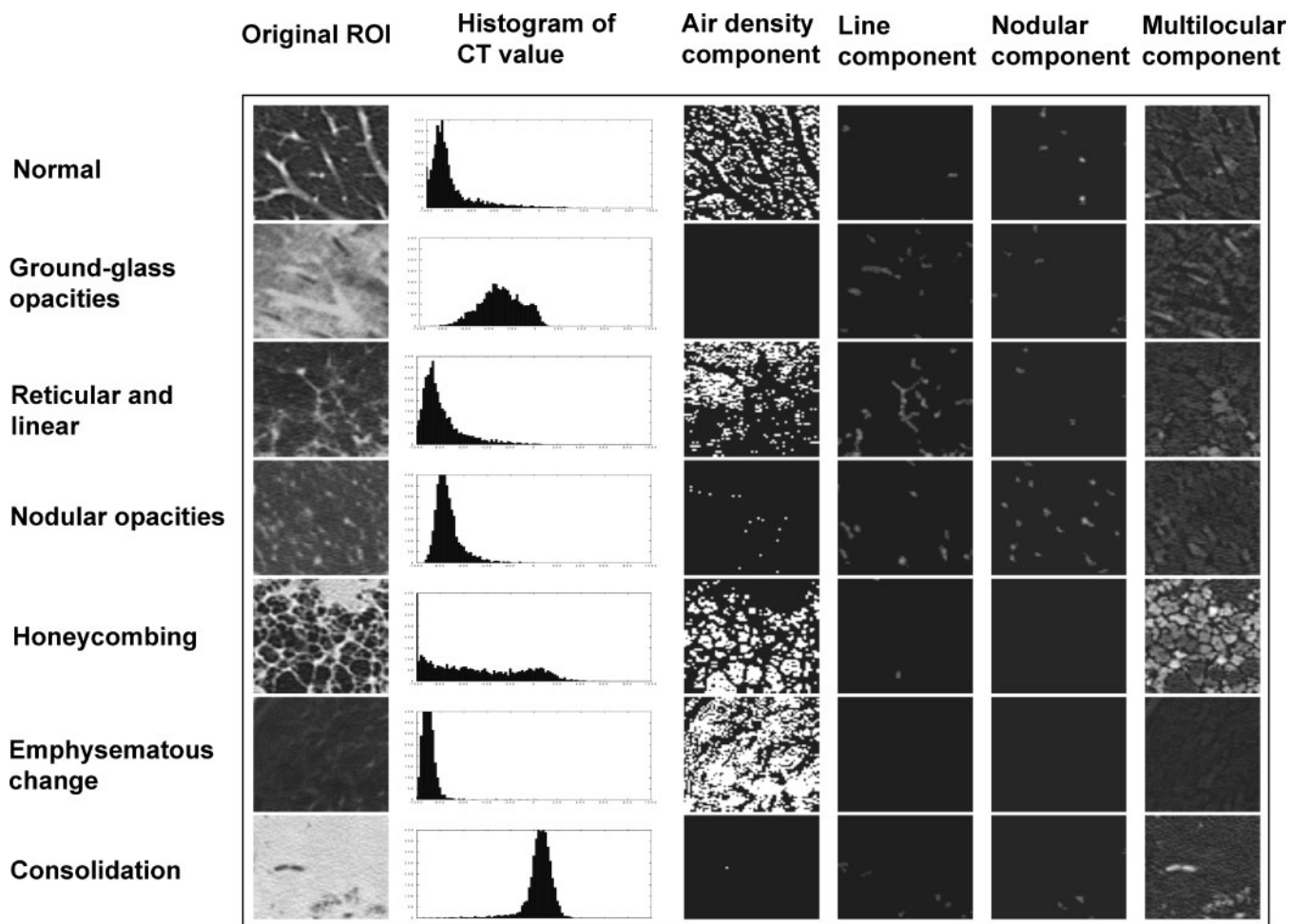


Figure 13. Illustration of images (96×96) selected from the seven slices in Figure 12, histograms of region-of-interest (ROI) images, and output images for air density components, line components, nodular components and multilocular components.

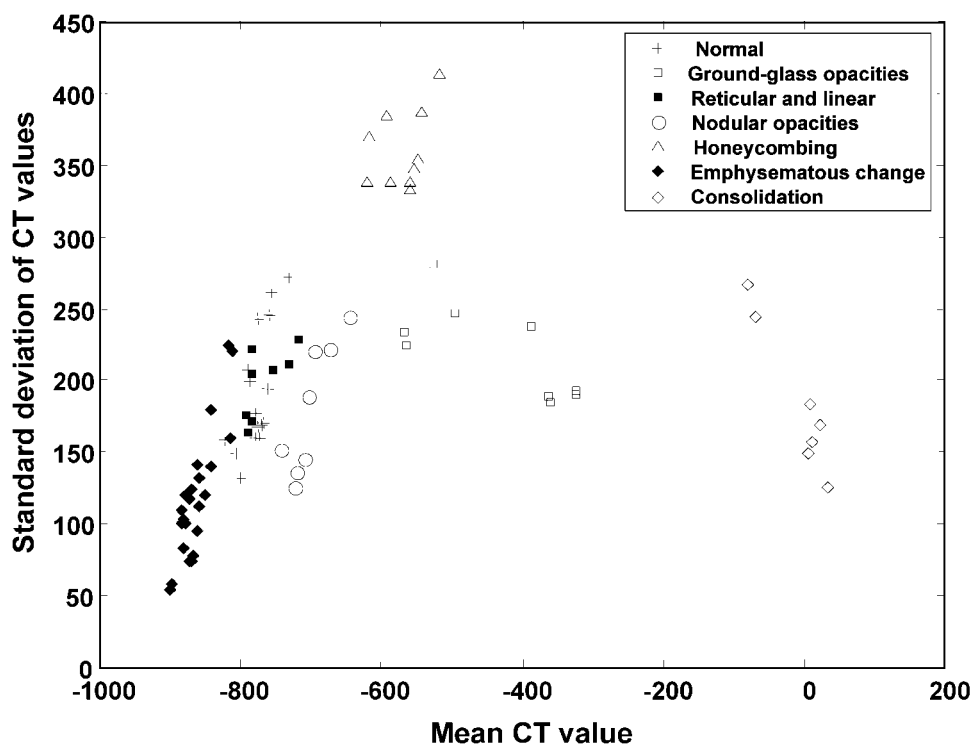
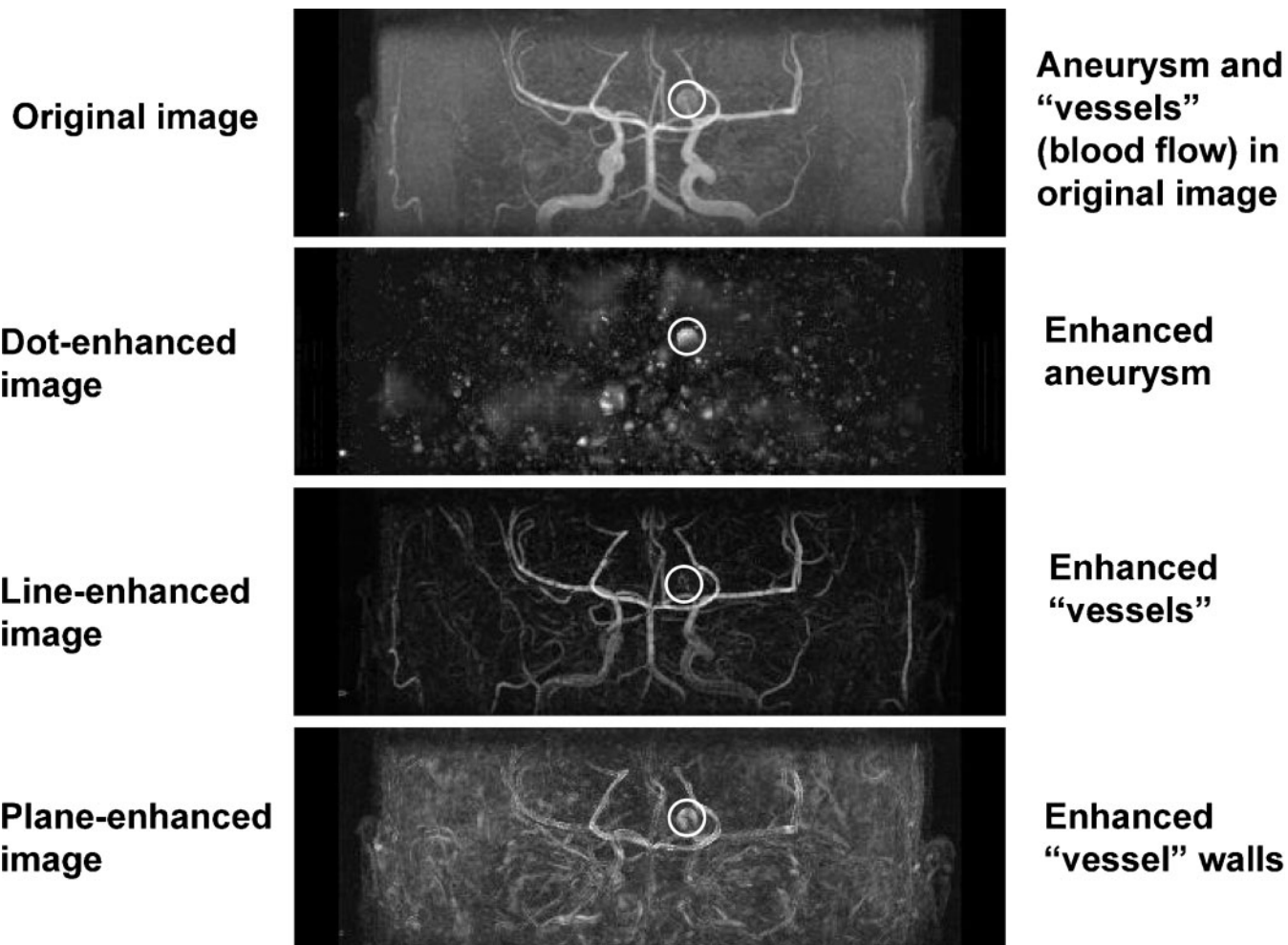
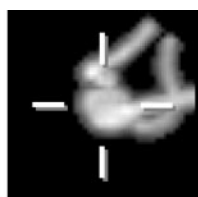


Figure 14. Illustration of the distribution of mean CT values and the standard deviation of CT values for six abnormal patterns and normals on high resolution CT.



**Figure 15.** Illustration of an original magnetic resonance angiography (MRA) image and three images selectively enhanced for dot, line, and plane objects, all of which were produced by maximum intensity projection (MIP) image processing. Circles indicate a large (7.5 mm) aneurysm.



**Aneurysm**

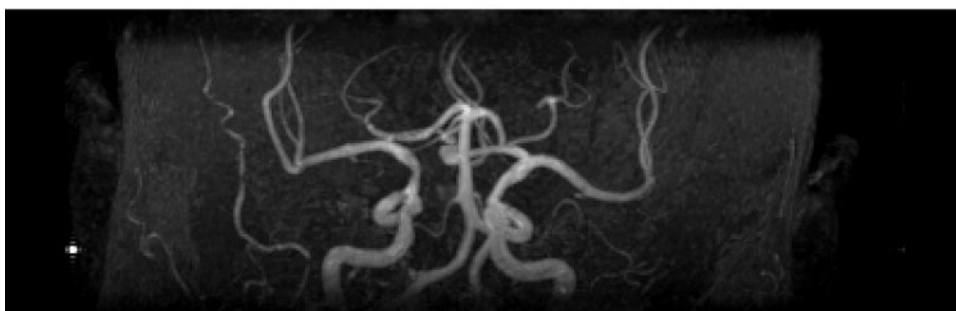


**Figure 16.** An original magnetic resonance angiography (MRA) image and an enlarged aneurysm detected by computer.

patients, which included normal and abnormal slices related to six different patterns, *i.e.* GGOs, reticular and linear opacities, nodular opacities, honeycombing, emphysematous change and consolidation. The areas that included specific diffuse patterns in the 315 HRCT images were marked by three radiologists independently on the CRT monitor in the same manner to how they commonly describe them in their radiological reports. The areas with a specific pattern, which three radiologists marked independently and consistently as the same patterns, were used as “gold standard” for specific abnormal opacities in this study, as illustrated in Figure 12.

In our CAD scheme developed by Uchiyama et al [110], the lungs were first segmented from background in each slice by use of a morphological filter and a thresholding technique, and were then divided into many contiguous ROIs with a  $32 \times 32$  (and/or  $96 \times 96$ ) matrix. Six physical measures that were determined in each ROI included the mean and the standard deviation of the CT value, air density components, nodular components, line components and multilobar components [110], as illustrated in Figure 13. The distribution of two of the physical measures is shown in Figure 14, where some of the six different patterns listed above can be clearly distinguished even with the use of only two physical measures. ANNs were employed for distinguishing between seven different patterns, which included normals and the six patterns associated with diffuse lung disease. The sensitivity of this computerised method for detection of the six abnormal patterns in each ROI was 99.2% (122/123) for GGOs, 100% (15/15) for reticular and linear opacities, 88.0% (132/150) for nodular opacities, 100% (98/98) for honeycombing, 95.8% (369/385) for emphysematous change and 100% (43/43) for consolidation. The specificity in detecting a normal ROI was 88.1% (940/1067). Therefore, this computerised method may be useful in assisting radiologists in their assessment of diffuse lung disease on HRCT images.

### Detection of intracranial aneurysms on magnetic resonance angiography

Prospective autopsy and angiographic studies indicated that between 3.6% and 6% of the general population have intracranial aneurysms [111] that could cause a subarachnoid haemorrhage (SAH) due to rupture of the aneurysm [112]. SAH is a serious disorder with high mortality and morbidity [113–116] (approximately 40–50% mortality rate) [113, 117]. The rate of rupture of asymptomatic aneurysms was estimated to be 1–2% per year [111, 118]. During the past decade, there has been considerable interest in the roles of “less invasive” imaging modalities such as computed tomographic angiography (CTA) and magnetic resonance angiography (MRA) in the detection of intracranial aneurysms [111, 119–125]. However, it is still difficult and time consuming for radiologists to find small aneurysms, or it may not be easy to detect even medium-sized aneurysms on maximum intensity projection (MIP) images because of overlap with adjacent vessels and unusual locations. Therefore, a CAD scheme would be useful in assisting radiologists in the detection of intracranial aneurysms, especially small aneurysms, by use of MRA.

Recently, Arimura et al [126, 127] have developed a computerised scheme for automated detection of unruptured intracranial aneurysms in MRA based on the use of a 3D selective enhancement filter [128] for dots (aneurysms). 29 cases with 36 unruptured aneurysms (diameter 3–26 mm, mean 6.6 mm) and 31 non-aneurysm cases were used in this study. The isotropic 3D-MRA images with  $400 \times 400 \times 128$  voxels (a voxel size of 0.5 mm) were processed by use of a selective, multiscale enhancement filter [128], as illustrated in Figure 15. The initial candidates were identified by use of a multiple grey-level thresholding technique on the dot-enhanced images and a region-growing technique with monitoring of some image features. All candidates were classified into four types according to the size and local structures based on the effective diameter and the skeleton image of each candidate, *i.e.* large candidates and three types of small candidates – a short-branch type a single-vessel type and a bifurcation type. In each group, a number of false positives were removed by use of different rules on localised image features related to grey levels and morphology. LDA was employed for further removal of false positives. With our CAD scheme, each of the 36 aneurysms was correctly detected, with 2.4 false positives per patient based on a leave-one-out-by-patient test method. Therefore, our CAD system would be useful in assisting radiologists in the detection of intracranial aneurysms in MRA. Our preliminary study on the effect of the computer output on radiologists’ detection performance indicated that the ROC curve for radiologists in the detection of intracranial aneurysms in MRA was improved when the computer output such as that illustrated in Figure 16 was available.

### Conclusion

A number of CAD schemes have been developed for detection and classification of lesions in medical images. Observer performance studies indicated that the computer output helped radiologists to improve their diagnostic accuracy. Because CAD can be applied to all imaging modalities, all body parts and all kinds of examinations, it is likely that CAD will have a major impact on medical imaging and diagnostic radiology in the 21st century.

### Acknowledgments

The author is grateful to more than 100 individuals, including the faculty, research associates, fellows, residents, research staff, international visitors and graduate students in the Department of Radiology, The University of Chicago, who have contributed to research on and development of CAD schemes over the last two decades; and to Mrs E Lanzl for improving the manuscript. This study was supported by USPHS Grants CA 61625 and CA 98119. KD is a shareholder of R2 Technology, Inc., Los Altos, CA, and Deus Technologies, Inc., Rockville, MD. CAD technologies developed in the Kurt Rossmann Laboratories have been licensed to companies including R2 Technology, Deus Technologies, Mitsubishi Space Software Co., General Electric Corporation, Median Technologies and Toshiba Corporation. It is the policy of The University of Chicago that investigators disclose

publicly actual or potential significant financial interests that may appear to be affected by research activities.

## References

- Doi K, Giger ML, MacMahon H, et al. Computer-aided diagnosis: development of automated schemes for quantitative analysis of radiographic images. *Sem Ultrasound CT MR* 1992;13:140–52.
- Doi K, Giger ML, Nishikawa RM, Hoffmann KR, MacMahon H, Schmidt RA, et al. Digital radiography: a useful clinical tool for computer-aided diagnosis by quantitative analysis of radiographic images. *Acta Radiol* 1993;34:426–39.
- Doi K, MacMahon H, Giger ML, Hoffmann KR, editors. *Computer aided diagnosis in medical imaging*. Elsevier, Amsterdam, 1999:3–560.
- Doi K, MacMahon H, Katsuragawa S, Nishikawa RM, Jiang Y. Computer-aided diagnosis in radiology: potential and pitfalls. *Eur J Radiol* 1999;31:97–109.
- Doi K. Present status and future horizons for computer-aided diagnosis in radiology. In: Sharp PE, Perkins AC, editors. *Physics and engineering in medicine in the new millennium*. London, UK: Institute of Physics and Engineering in Medicine, 2000:84–7.
- Doi K. Computer-aided diagnosis in radiology: basic concept, current status and future potential. In: Xie N-Z, editor. *Medical imaging and precision radiotherapy*. Guangzhou, China: Foundation of International Scientific Exchange, 2000:125–38.
- Giger ML, Huo Z, Kupinski MA, Vyborny CJ. Computer-aided diagnosis in mammography. In: Fitzpatrick JM, Sonka M, editors. *The handbook of medical imaging*, Vol. 2. Medical imaging processing and analysis. Bellingham, WA: SPIE, 2000:915–1004.
- Erickson BJ, Bartholmai B. Computer-aided detection and diagnosis at the start of the third millennium. *J Digit Imaging* 2002;15:59–68.
- Summers RM. Road maps for advancement of radiologic computer-aided detection in the 21<sup>st</sup> century. *Radiology* 2003;229:11–3.
- Doi K. Computer-aided diagnosis in digital chest radiography. *Advances in Digital Radiography*, RSNA categorical course in Diagnostic Radiology: Physics Syllabus. Oak Brook, IL: RSNA, 2003:227–36.
- Abe H, MacMahon H, Engelmann R, Li Q, Shiraishi J, Katsuragawa S, et al. Computer-aided diagnosis in chest radiology: results of large-scale observer tests performed at the 1996–2001 RSNA Scientific Assemblies. *RadioGraphics* 2003;23:255–65.
- Dodd LE, Wagner RF, Armato SG, McNitt-Gray MF, et al. Assessment of methodologies and statistical issues for computer-aided diagnosis of lung nodules in computed tomography: contemporary research topics relevant to the lung image database consortium. *Acad Radiol* 2004;11:462–75.
- Gur D, Zhang B, Fuhrman CR, Hardesty L. On the testing and reporting of computer-aided detection results for lung cancer detection. *Radiology* 2004;232:5–6.
- Lodwick GS, Haun CL, Smith WE, et al. Computer diagnosis of primary bone tumor. *Radiology* 1963;80:273–5.
- Myers PH, Nice CM, Becker HC, et al. Automated computer analysis of radiographic images. *Radiology* 1964;83:1029–33.
- Winsberg F, Elkin M, May J, et al. Detection of radiographic abnormalities in mammograms by means of optical scanning and computer analysis. *Radiology* 1967;89:211–5.
- Kruger RP, Towns JR, Hall DL, et al. Automated radiographic diagnosis via feature extraction and classification of cardiac size and shape descriptors. *IEEE Trans Biomed Eng* 1972;19:174–86.
- Kruger RP, Thompson WB, Turner AF. Computer diagnosis of pneumoconiosis. *IEEE Transactions on Systems, Man, and Cybernetics*, 1974;4.
- Toriwaki J, Suenaga Y, Negoro T, et al. Pattern recognition of chest x-ray images. *Computer Graphics and Image Processing* 1973;2:252–71.
- Engle RL. Attempt to use computers as diagnostic aids in medical decision making: a thirty-year experience. *Perspect Biol Med* 1992;35:207–19.
- Chan HP, Doi K, Galhotra S, Vyborny CJ, MacMahon H, Jokich PM. Image feature analysis and computer-aided diagnosis in digital radiography. 1. Automated detection of microcalcifications in mammography. *Med Phys* 1987;14:538–48.
- Chan HP, Doi K, Vyborny CJ, Schmidt RA, Metz CE, Lam KL, et al. Improvement in radiologists' detection of clustered microcalcifications on mammograms: the potential of computer-aided diagnosis. *Invest Radiol* 1990;25:1102–10.
- Yin FF, Giger ML, Doi K, Metz CE, Vyborny CJ, Schmidt RA. Computerized detection of masses in digital mammograms: analysis of bilateral subtraction images. *Med Phys* 1991;18:955–63.
- Kegelmeyer WP, Pruneda JM, Bourland PD, Hillis A, Riggs MW, Nipper ML. Computer-aided mammographic screening for spiculated lesions. *Radiology* 1994;191:331–7.
- Huo Z, Giger ML, Vyborny CJ, Wolverton DE, Schmidt RA, Doi K. Automated computerized classification of malignant and benign mass lesions on digitized mammograms. *Acad Radiol* 1998;15:155–68.
- Jiang Y, Nishikawa RM, Schmidt RA, Metz CE, Giger ML, Doi K. Improving breast cancer diagnosis with computer-aided diagnosis. *Acad Radiol* 1999;6:22–33.
- Warren-Burhenne LJ, Wood SA, D'Orsi CJ, et al. Potential contribution of computer-aided detection to the sensitivity of screening mammography. *Radiology* 2000;215:554–62.
- Jiang Y, Nishikawa RM, Schmidt RA, Toledano AY, Doi K. The potential of computer-aided diagnosis (CAD) to reduce variability in radiologists' interpretation of mammograms containing microcalcifications. *Radiology* 2001;220:787–94.
- Freer TW, Ulissey MJ. Screening mammography with computer-aided detection: prospective study of 12,860 patients in a community breast center. *Radiology* 2001;220:781–6.
- Schmidt RA, Nishikawa RM, Osnis RB, Schreiberman K, Giger ML, Doi K. Computerized detection of lesions missed by mammography. In: Doi K, Giger ML, Nishikawa RM, Schmidt RA, editors. *Digital mammography*. Amsterdam, The Netherlands: Elsevier Science, 1996:105–10.
- Giger ML, Doi K, MacMahon H. Image feature analysis and computer-aided diagnosis in digital radiography. 3. Automated detection of nodules in peripheral lung fields. *Med Phys* 1988;15:158–66.
- Xu XW, Doi K, Kobayashi T, MacMahon H, Giger ML. Development of an improved CAD scheme for automated detection of lung nodules in digital chest images. *Med Phys* 1997;24:1395–403.
- Kobayashi T, Xu XW, MacMahon H, Metz CE, Doi K. Effect of a computer-aided diagnosis scheme on radiologists' performance in detection of lung nodules on radiographs. *Radiology* 1996;199:843–8.
- Katsuragawa S, Doi K, MacMahon H. Image feature analysis and computer-aided diagnosis in digital radiography: detection and characterization of interstitial lung disease in digital chest radiographs. *Med Phys* 1988;15:311–9.

35. Ishida T, Katsuragawa S, Nakamura K, Ashizawa K, MacMahon H, Doi K. Computerized analysis of interstitial lung diseases on chest radiographs based on lung texture, geometric-pattern features and artificial neural networks. *Proc SPIE* 2002;4684:1331–8.
36. Monnier-Cholley L, MacMahon H, Katsuragawa S, Morishita J, Ishida T, Doi K. Computer aided diagnosis for detection of interstitial infiltrates in chest radiographs: evaluation by means of ROC analysis. *AJR* 1998;171:1651–6.
37. Ashizawa K, Ishida T, MacMahon H, Vyborny CJ, Katsuragawa S, Doi K. Artificial neural networks in chest radiographs: application to differential diagnosis of interstitial lung disease. *Acad Radiol* 1999;6:2–9.
38. Ashizawa K, MacMahon H, Ishida T, Nakamura K, Vyborny CJ, Katsuragawa S, et al. Effect of an artificial neural network on radiologists' performance of differential diagnoses of interstitial lung disease using chest radiographs. *AJR* 1999;172:1311–5.
39. Kano A, Doi K, MacMahon H, Hassell DD, Giger ML. Digital image subtraction of temporally sequential chest images for detection of interval change. *Med Phys* 1994;21:453–61.
40. Ishida T, Katsuragawa S, Nakamura K, MacMahon H, Doi K. Iterative image warping technique for temporal subtraction of sequential chest radiographs to detect interval change. *Med Phys* 1999;26:1320–9.
41. Li Q, Katsuragawa S, Doi K. Improved contralateral subtraction images by use of elastic matching technique. *Med Phys* 2000;27:1934–42.
42. Difazio MC, MacMahon H, Xu XW, Tsai P, Shiraishi J, Armato SG, et al. Effect of time interval difference images on detection accuracy in digital chest radiography. *Radiology* 1997;202:447–52.
43. Uozumi T, Nakamura K, Watanabe H, Nakata H, Katsuragawa S, Doi K. ROC analysis on detection of metastatic pulmonary nodules on digital chest radiographs by use of temporal subtraction. *Acad Radiol* 2001;8:871–8.
44. Kakeda S, Nakamura K, Kamada K, Watanabe H, Nakata H, Katsuragawa S, et al. Observer performance study on the usefulness of temporal subtraction in detection of lung nodules on digital chest images. *Radiology* 2002;224:145–51.
45. Nakamori N, Doi K, MacMahon H, Sasaki Y, Montner S. Effect of heart size parameters computed from digital chest radiographs on detection of cardiomegaly: potential usefulness for computer-aided diagnosis. *Invest Radiol* 1991;26:546–50.
46. Sanada S, Doi K, MacMahon H. Image feature analysis and computer-aided diagnosis in digital radiography: automated detection of pneumothorax in chest images. *Med Phys* 1992;19:1153–60.
47. Nakamura K, Yoshida H, Engelmann R, MacMahon H, Katsuragawa S, Ishida T, et al. Computerized analysis of the likelihood of malignancy in solitary pulmonary nodules by use of artificial neural networks. *Radiology* 2000;214:823–30.
48. Aoyama M, Li Q, Katsuragawa S, MacMahon H, Doi K. Automated computerized scheme for distinction between benign and malignant solitary pulmonary nodules on chest images. *Med Phys* 2002;29:701–8.
49. Shiraishi J, Abe H, Engelmann R, Aoyama M, MacMahon H, Doi K. Computer-aided diagnosis for distinction between benign and malignant solitary pulmonary nodules in chest radiographs: ROC analysis of radiologists' performance. *Radiology* 2003;227:469–74.
50. Giger ML, Bae KT, MacMahon H. Computerized detection of pulmonary nodules in CT images. *Invest Radiol* 1994;29:459–65.
51. Armato SG III, Giger ML, MacMahon H. Automated detection of lung nodules in CT scans: preliminary results. *Med Phys* 2001;28:1552–61.
52. Armato SG III, Li F, Giger ML, MacMahon H, Sone S, Doi K. Performance of automated CT nodule detection on missed cancers from a lung cancer screening program. *Radiology* 2002;225:685–92.
53. Jiang H, Yamamoto S, Iisaku S, et al. Computer-aided diagnosis system for lung cancer screening by CT. In: Doi K, et al, editors. *Computer-aided diagnosis in medical imaging*. Amsterdam, The Netherlands: Elsevier, 1999:125–30.
54. Ukai Y, Niki N, Satoh H, et al. Computer aided diagnosis system for lung cancer based on retrospective helical CT image. *Proc. SPIE* 2000;3979:1028–39.
55. Armato III SG, Giger ML, Moran CJ, et al. Computerized detection of pulmonary nodules on CT scans. *Radiographics* 1999;19:1303–11.
56. Lawler LP, Wood SA, Paunu HS, Fishman EK. Computer-assisted detection of pulmonary nodules: preliminary observations using a prototype system with multidetector-row CT data sets. *J Digit Imaging* 2003;16:251–61.
57. Wormanns D, Fiebich M, Saidi M, et al. Automatic detection of pulmonary nodules at spiral CT: clinical application of a computer-aided diagnosis system. *Eur Radiol* 2002;12:1052–7.
58. Gurcan MN, Sahiner B, Petrick N, et al. Lung nodule detection on thoracic computed tomography images: Preliminary evaluation of a computer-aided diagnosis system. *Med Phys* 2002;29:2552–8.
59. Brown MS, Goldin JG, Suh RD, et al. Lung micronodules: automated method for detection at thin-section CT – initial experience. *Radiology* 2003;226:256–62.
60. Suzuki K, Armato III SG, Li F, et al. Massive training artificial neural network (MTANN) for reduction of false positives in computerized detection of lung nodules in low-dose CT. *Med Phys* 2003;30:1602–17.
61. Okumura T, Miwa, T, Kako J, Yamamoto S, Matsumoto M, Tateno Y, et al. Variable N-Quoit filter applied for automatic detection of lung cancer by X-ray CT. In: Lemke HU, Vannier MW, Inamura K, Farman A, editors. *Computer-assisted radiology*. Amsterdam, The Netherlands: Elsevier Science, 1998:242–7.
62. Lee Y, Hara T, Fujita H, Itoh S, Ishigaki T. Automated detection of pulmonary nodules in helical CT images based on an improved template-matching technique. *IEEE Trans Med Imaging* 2001;20:595–604.
63. Kanazawa K, Kawata Y, Niki N, Satoh H, Ohmatsu H, Kakinuma R, et al. Computer aided diagnostic system for pulmonary nodules based on helical CT images. In: Doi K, MacMahon H, Giger ML, Hoffmann KR, editors. *Computer-aided diagnosis in medical imaging*. Amsterdam, The Netherlands: Elsevier Science, 1999:131–6.
64. Brown MS, McNitt-Gray MF, Goldin JG, Suh RD, Sayre JW, Aberle DR. Patient-specific models for lung nodule detection and surveillance in CT images. *IEEE Trans Med Imaging* 2001;20:1242–50.
65. McNitt-Gray MF, Hart EM, Wyckoff N, et al. A pattern classification approach to characterizing solitary pulmonary nodules imaged on high resolution CT: preliminary results. *Med Phys* 1999;26:880–8.
66. Wyckoff N, McNitt-Gray MF, Goldin JG, et al. Classification of solitary pulmonary nodules (SPNs) imaged on high resolution CT using contrast enhancement and three dimensional quantitative image features. *Proc. SPIE* 2000;3979:1107–15.
67. McNitt-Gray MF, Wyckoff N, Goldin JG, et al. Computer-aided diagnosis of the solitary pulmonary nodule imaged on CT: 2D, 3D and contrast enhancement features. *Proc. SPIE* 2001;4322:1845–52.
68. Kawata Y, Niki N, Ohmatsu H, et al. Classification of pulmonary nodules in thin section CT images based on shape characterization. *Proc. ICIP* 1997;3:528–31.

69. Kawata Y, Niki N, Ohmatsu H, et al. Example-based assisting approach for pulmonary nodule classification in three-dimensional thoracic computed tomography images. *Acad Radiol* 2003;10:1402–15.
70. Awai K, Murao K, Ozawa A, et al. Pulmonary nodules at chest CT: effect of computer-aided diagnosis on radiologists' detection performance. *Radiology* 2004;230:347–52.
71. McCulloch CC, Kaucic RA, Mendonca PRS, et al. Model-based detection of lung nodules in computed tomography exams. *Acad Radiol* 2004;11:258–66.
72. Yoshida H, Näppi J, MacEneaney P, Rubin D, Dachman AH. Computer-aided diagnosis scheme for the detection of polyps with CT colonography. *Radiographics* 2002;22:963–79.
73. Yoshida H, Masutani Y, MacEneaney P, Rubin D, Dachman AH. Computerized detection of colonic polyps at CT colonography on the basis of volumetric features: pilot study. *Radiology* 2002;222:327–36.
74. Yoshida H, Näppi J. Three-dimensional computer-aided diagnosis scheme for detection of colonic polyps. *IEEE Trans Med Imaging* 2001;20:1261–74.
75. Kiss G, Van Cleynenbreugel J, Thomeer M, Suetens P, Marchal G. Computer-aided diagnosis in virtual colonography via combination of surface normal and sphere fitting methods. *Eur Radiol* 2002;12:77–81.
76. Summers RM, Johnson CD, Pusanik LM, Malley JD, Youssef AM, Reed JE. Automated polyp detection at CT colonography: feasibility assessment in a human population. *Radiology* 2001;219:51–9.
77. Gokturk SB, Tomasi C, Acar B, et al. A statistical 3-D pattern processing method for computer-aided detection of polyps in CT colonography. *IEEE Trans Med Imaging* 2001;20:1251–60.
78. Acar B, Beaulieu CF, Gokturk SB, et al. Edge displacement field-based classification for improved detection of polyps in CT colonography. *IEEE Trans Med Imaging* 2002;21:1461–7.
79. Jerebko AK, Summers RM, Malley JD, Franaszek M, Johnson CD. Computer-assisted detection of colonic polyps with CT colonography using neural networks and binary classification trees. *Med Phys* 2003;30:52–60.
80. Jerebko AK, Malley JD, Franaszek M, Summers RM. Multiple neural network classification scheme for detection of colonic polyps in CT colonography data sets. *Acad Radiol* 2003;10:154–60.
81. Näppi J, Yoshida H. Feature-guided analysis for reduction of false positives in CAD of polyps for computed tomographic colonography. *Med Phys* 2003;30:1592–601.
82. Yoshida H, Dachman AH. CAD techniques, challenges, and controversies in CT colonography. *Abdom Imaging* 2005;30:24–39.
83. Brem R, Baum J, Lechner M, et al. Improvement in sensitivity of screening mammography with computer-aided detection: a multi-institutional trials. *AJR* 2003;181:687–93.
84. Sacks WM. Estimating the effect of computer-aided detection on the sensitivity of screening mammography. *Radiology* 2003;226:597–8.
85. Zheng B, Swensson RG, Golla S, et al. Detection and classification performance levels of mammographic masses under different computer-aided detection cueing environments. *Acad Radiol* 2004;11:396–406.
86. Ciatto S, Turco MR, Risso G, et al. Comparison of standard reading and computer-aided detection (CAD) on a national proficiency test of screening mammography. *Eur J Radiol* 2003;45:135–8.
87. Klym AH, King JL, Hardesty L. The effect of routine use of a computer-aided detection system on the practice of breast imagers: a subjective assessment. *Acad Radiol* 2004;11:711–3.
88. Ikeda DM, Birdwell RL, O'Shaughnessy KF, et al. Computer-aided detection output on 172 subtle findings on normal mammograms previously obtained in women with breast cancer detected at follow-up screening mammography. *Radiology* 2004;230:811–9.
89. Gur D, Sumkin JH, Rockette HE, et al. Changes in breast cancer detection and mammography recall rates after the introduction of a computer-aided detection system. *J Natl Cancer Inst* 2004;96:185–90.
90. Karssemeijer N, Risso G, Catarzi S, et al. Computer-aided detection versus independent double reading of masses on mammograms. *Radiology* 2003;227:192–200.
91. Kakeda S, Moriya J, Sato H, et al. Improved detection of lung nodules on chest radiographs using a commercial computer-aided diagnostic system. *AJR* 2004;182:505–10.
92. Kaneko M, Eguchi K, Ohmatsu H, et al. Peripheral lung cancer: screening and detection with low-dose spiral CT versus radiography. *Radiology* 1996;201:798–802.
93. Sone S, Takashima S, Li F, et al. Mass screening for lung cancer with mobile spiral computed tomography scanner. *Lancet* 1998;351:1242–5.
94. Henschke CI, McCauley DI, Yankelevitz DF, et al. Early lung cancer action project: overall design and findings from baseline screening. *Lancet* 1999;354:99–105.
95. Diederich S, Lenzen H, Windmann R, et al. Pulmonary nodules: experimental and clinical studies at low-dose CT. *Radiology* 1999;213:289–98.
96. Nawa T, Nakagawa T, Kusano S, et al. Lung cancer screening using low-dose spiral CT: results of baseline and 1-year follow-up studies. *Chest* 2002;122:15–20.
97. Swensen SJ, Jett JR, Hartman TE, et al. Lung cancer screening with CT: Mayo Clinic experience. *Radiology* 2003;226:756–61.
98. Diederich S, Wormanns D, Semik M, Thomas M, Lenzen H, Roos N, et al. Screening for early lung cancer with low-dose spiral CT: prevalence in 817 asymptomatic smokers. *Radiology* 2002;222:773–81.
99. Swensen SJ, Jett JR, Sloan JA, Midthun DE, Hartman TE, Sykes AM, et al. Screening for lung cancer with low-dose spiral computed tomography. *Am J Respir Crit Care Med* 2002;165:508–13.
100. Mahadevia PJ, Fleisher LA, Frick KD, Eng J, Goodman SN, Powe NR. Lung cancer screening with helical computed tomography in older adult smokers. *JAMA* 2003;289:313–22.
101. Li F, Sone S, Abe H, et al. Lung cancers missed at low-dose helical CT screening in a general population: comparison of clinical, histopathologic, and imaging findings. *Radiology* 2002;225:673–83.
102. Arimura H, Katsuragawa S, Suzuki K, Li F, Shiraishi J, Doi K. Computerized scheme for automated detection of lung nodules in low-dose CT images for lung cancer screening. *Acad Radiol* 2004;11:617–29.
103. Suzuki K, Armato III SG, Li F, et al. Effect of a small number of training cases on the performance of massive training artificial neural network (MTANN) for reduction of false positives in computerized detection of lung nodules in low-dose CT. *Proc. SPIE* 2003;5032:1355–66.
104. Li F, Arimura H, Shiraishi J, Sone S, MacMahon H, Doi K. Computer-aided diagnosis for detection of subtle peripheral lung cancers on CT: an ROC and LROC analysis. Presented at the 89th meeting of the Radiological Society of North America. Annual Meeting Program, 2003:292.
105. Aoyama M, Li Q, Katsuragawa S, Li F, Sone S, Doi K. Computerized scheme for determination of the likelihood measure of malignancy for pulmonary nodules on low-dose CT images. *Med Phys* 2003;30:387–94.

106. Li F, Aoyama M, Shiraishi J, Abe H, Li Q, Suzuki K, et al. Improvement in radiologists' performance for differentiating small benign from malignant lung nodules on high-resolution CT by using computer-estimated likelihood of malignancy. *AJR* 2004;183:1209–15.
107. Li Q, Li F, Katsuragawa S, Shiraishi J, MacMahon H, Sone S, et al. Investigation of new psychophysical measures for evaluation of similar images on thoracic computed tomography for distinction between benign and malignant nodules. *Med Phys* 2003;30:2584–93.
108. Sone S, Li F, Yang Z, Takashima S, Maruyama Y, Hasegawa Wang M, et al. Characteristics of small lung cancers invisible on conventional chest radiography: analysis of 44 lung cancers detected by population-based screening using low-dose spiral CT. *Br J Radiol* 2000;73:137–45.
109. Sone S, Li F, Yang Z, Honda T, Maruyama Y, Takashima S, et al. Results of three-year mass screening programme for lung cancer using mobile low-dose spiral computed tomography scanner. *Br J Cancer* 2001;84:25–32.
110. Uchiyama Y, Katsuragawa S, Abe H, Shiraishi J, Li F, Li Q, et al. Quantitative computerized analysis of diffuse lung disease in high-resolution computed tomography. *Med Phys* 2003;30:2440–64.
111. Wardlaw JM, White PM. The detection and management of unruptured intracranial aneurysms. *Brain* 2000;123:205–21.
112. Weir B. Unruptured intracranial aneurysms: a review. *J Neurosurg* 2002;96:3–42.
113. Fogelholm R, Hernesniemi J, Vapalahti M. Impact of early surgery on outcome after aneurysm subarachnoid hemorrhage: a population-based study. *Stroke* 1993;24:1649–54.
114. Hop JW, Rinkel GJ, Algra A, van Gijn J. Case-fatality rates and functional outcome after subarachnoid hemorrhage: a systematic review. *Stroke* 1997;28:660–4.
115. Hijdra A, Braakman R, van Gijn J, Vermeulen M, van Crevel H. Aneurysmal subarachnoid hemorrhage: complications and outcome in a hospital population. *Stroke* 1987;18:1061–7.
116. Sengupta RP, McAllister V. Subarachnoid hemorrhage. Berlin, Germany: Springer-Verlag, 1986.
117. Broderick JP, Brott TG, Duldner JE, Tomsick T, Leach A. Initial and recurrent bleeding are the major causes of death following subarachnoid hemorrhage. *Stroke* 1994;25:1342–7.
118. Juvela S, Porras M, Poussa K. Natural history of unruptured intracranial aneurysms: probability of and risk factors for aneurysm rupture. *J Neurosurg* 2000;93:379–87.
119. Ogawa T, Okudera T, Noguchi K, Sasaki N, Inugami A, Uemura K, et al. Cerebral aneurysms: evaluation with three-dimensional CT angiography. *Am J Neuroradiol* 1996;17:447–54.
120. Korogi Y, Takahashi M, Katada K, Ogura Y, Hasuo K, Ochi M, et al. Intracranial aneurysms: detection with three-dimensional CT angiography with volume rendering – comparison with conventional angiographic and surgical findings. *Radiology* 1999;211:497–506.
121. White PM, Teasdale EM, Wardlaw JM, Easton V. Intracranial aneurysms: CT angiography and MR angiography for detection – prospective blinded comparison in a large patient cohort. *Radiology* 2001;219:739–49.
122. Preda L, Gaetani P, Rodriguez y Baena R, Di Maggio EM, La Fianza A, Dore R, et al. Spiral CT angiography and surgical corrections in the evaluation of intracranial aneurysms. *Eur Radiol* 1998;8:739–45.
123. Huston J III, Nichols DA, Luetmer PH, Goodwin JT, Meyer FB, Wiebers DO, et al. Blinded prospective evaluation of sensitivity of MR angiography to known intracranial aneurysms: importance of aneurysm size. *Am J Neuroradiol* 1994;15:1607–14.
124. Aprile I. Evaluation of cerebral aneurysms with MR-angiography. *Riv Neuroradiol* 1996;9:541–50.
125. Korogi Y, Takahashi M, Mabuchi N, Miki H, Fujiwara S, Horikawa Y, et al. Intracranial aneurysms: diagnostic accuracy of three-dimensional, Fourier transform, time-of-flight MR angiography. *Radiology* 1994;193:181–6.
126. Arimura H, Li Q, Korogi Y, Hirai T, Abe H, Yamashita Y, et al. Development of CAD scheme for automated detection of intracranial aneurysms in magnetic resonance angiography. In: Lemke HU, et al, editors. *CARS 2004: Computer Assisted Radiology and Surgery. Proceedings of the 18th International Congress and Exhibition; 2004 June 23–26; Chicago, IL. Amsterdam, The Netherlands: Elsevier, 2004:1015–20.*
127. Arimura H, Li Q, Korogi Y, Hirai T, Abe H, Yamashita Y, et al. Automated computerized scheme for detection of unruptured intracranial aneurysms in three-dimensional magnetic resonance angiography. *Acad Radiol* 2004;11:1093–104.
128. Li Q, Sone S, Doi K. Selective enhancement filters for nodules, vessels, and airway walls in two- and three-dimensional CT scans. *Med Phys* 2003;30:2040–51.